Circular RNA expression profiles significantly altered in UVA-irradiated human dermal fibroblasts

MENGBI LIN, YUE ZHENG, QIAN LI, YUFANG LIU, QINGFANG XU, YUYING LI and WEI LAI

Department of Dermatology and Venereology, The Third Affiliated Hospital of Sun Yat-sen University, Guangzhou, Guangdong 510630, P.R. China

Received January 30, 2020; Accepted May 20, 2020

DOI: 10.3892/etm.2020.9292

Abstract. Circular RNAs (circRNAs) have been previously implicated in number of diseases. However, the roles of circRNAs in photoaging remain elusive. In the present study, to understand if photoaging influences the levels of circRNA expression, the expression of circRNAs in ultraviolet A (UVA)-irradiated human dermal fibroblasts were profiled. A total of 128 circRNAs were identified to be differentially expressed (fold change >1.5; P<0.05) after UVA exposure, including 39 upregulated and 89 downregulated circRNAs. Gene Ontology and Kyoto Encyclopedia of Genes and Genomes biological pathway analyses indicated that the differentially expressed circRNAs were associated with extracellular matrix organization and metabolism. The present study revealed an altered circRNA expression pattern in human dermal fibroblasts following UVA-irradiation. These results provide not only a basis for in-depth study of the mechanism of skin photoaging but also a new possibility for the prevention and treatment of photoaging and associated skin diseases.

Introduction

Ultraviolet A (UVA) radiation, which penetrates deep into the dermis and affects human dermal fibroblasts (HDFs), has an important role in inducing photoaging (1). The histopathological changes of photoaging are mainly manifested by the reduction of collagens and the denaturation and accumulation of elastic fibers (1,2). UVA not only affects the appearance of the skin, but also causes a variety of light-associated diseases, including actinic granuloma, squamous cell carcinoma and malignant melanoma (1,3-5).

Correspondence to: Dr Wei Lai, Department of Dermatology and Venereology, The Third Affiliated Hospital of Sun Yat-sen University, 600 Tianhe Road, Shipai Street, Guangzhou, Guangdong 510630, P.R. China
E-mail: drlaiwei@163.com

Key words: circular RNA, microRNA, photoaging, ultraviolet A, fibroblast, extracellular matrix

Although the mechanism of photoaging remains to be fully elucidated, there have been numerous advances in recent years. For example, microRNA (miR)-377 have been reported to promote the senescence of human dermal fibroblasts by targeting DNA methyltransferase (6), whilst the long noncoding RNA (lncRNA) RP11-670E13.6 delays the senescence of UVB-irradiated dermal fibroblasts by sponging microRNA-663a (7). These previous studies have emphasized the essential roles of non-coding RNAs in photoaging.

Circular (circ)RNAs, in contrast to conventional linear RNAs, are a class of non-coding RNAs formed by reverse splicing, without a 5' cap and a 3' polyA tail (8). Compared with other biomolecules, circRNAs are durable and stable functional molecules that do not get degraded (9). circRNAs bind miRNAs with complementary sequences through base-pair binding, thus acting like a sponge to regulate the expression of miRNA target genes (10).

It has been previously reported that circRNAs are involved in the development and progression of various diseases, including heart failure, cancer and Alzheimer disease (11-13). However, the role of circRNAs in photoaging remains to be fully elucidated. Therefore, the present study explored the expression profiles of circRNAs in ultraviolet A (UVA)-irradiated human dermal fibroblasts compared with those in the non-irradiated control group.

Materials and methods

Cell culture and UVA irradiation. The present study was approved by the Medical Ethics Committee of the Third Affiliated Hospital of Sun Yat-sen University (Guangzhou, China). The foreskin dermis of six healthy children aged from 3 to 9 years (7.00±1.63 years) was used to isolate and culture fibroblasts using procedures previously described (14). Cells were cultured in Dulbecco's modified Eagle's medium (Gibco; Thermo Fisher Scientific, Inc.) supplemented with 100 U/ml penicillin (Sigma-Aldrich; Merck KGaA;), 100 U/ml streptomycin (Sigma-Aldrich; Merck KGaA) and 10% fetal bovine serum (PAN-Biotech GmbH) in a 37˚C humidified incubator with 5% CO_2. Cells between the 4 and 6th passages were utilized for the assays. When the fibroblasts were in the exponential growth phase and their density reached 70%, cells were exposed to UVA irradiation, and control cells were treated under the same conditions but without UVA exposure. The radiation device was

a UVA lamp with a wavelength of 320-400 nm (Sigma-Aldrich; Merck KGaA), and the UVA dose was measured using a UVX digital radiometer (Shenzhen Sunkun Technology Co., Ltd.). The daily dose was 10 J/cm^2 (15). After 14 days of UVA irradiation, cells were harvested for subsequent experiments.

Confirmation of establishment of UVA-irradiated HDF model of ageing. A Senescence-Associated β-Galactosidase (SA-β-Gal) Staining kit (cat. no. C0602), purchased from Beyotime Institute of Biotechnology, was used to detect the senescent cells using manufacturer's protocol.

Detection of cell cycle-associated protein expression. Protein was extracted from cells using a Protein Extraction kit (Nanjing Keygen Biotech Co., Ltd.). The BCA Protein Assay kit (Thermo Fisher Scientific, Inc.) was used to detect the protein concentration. The protein (50 μg/lane) was separated by 12% SDS-PAGE and electro-transferred onto a 0.45-μm nitrocellulose membrane (EMD Millipore) for 90 min. The membrane was blocked with 5% bovine serum albumin (NeoFROXX GmbH) and incubated overnight at 4˚C on a shaker with the following monoclonal primary antibodies: Rabbit P21 (1:1,000 dilution; cat. no. 2947; Cell Signaling Technology, Inc.), rabbit P16 (1:1,000 dilution; cat. no. ab51243; Abcam) and mouse P53 (1:1,000 dilution; cat. no. 9282; Cell Signaling Technology, Inc.). Subsequently, the membrane was washed with TBS-T (0.05% Tween-20 in TBS; pH 7.4) and incubated with horseradish peroxidase-conjugated secondary antibodies (1:5,000 dilution; cat. nos. 7074 and 7076; Cell Signaling Technology, Inc.) for 1 h at room temperature and protein bands were visualized by chemiluminescence (ECL Advanced Detection Kit; EMD Millipore). GAPDH (1:1,000 dilution; cat. no. 2118; Cell Signaling Technology, Inc.) was used as an internal control. The band densities were measured using ImageJ software (version 1.50; National Institutes of Health).

RNA extraction and quality control. Total RNA was extracted from fibroblasts by TRIzol® reagent (Invitrogen; Thermo Fisher Scientific, Inc.) according to the manufacturer's protocol, and a NanoDrop ND-1000 (NanoDrop; Thermo Fisher Scientific, Inc.) was used to determine the purity and concentration of total RNA in the samples.

circRNA microarrays and bioinformatics analysis. Total RNAs from each sample were treated with RNase R (cat. no. M1228-500; BioVision, Inc.) to enrich circRNAs. Subsequently, referring to the Arraystar super RNA Labeling scheme (Arraystar, Inc.), the enriched circRNAs were amplified with random primers and transcribed into fluorescent complementary RNA (cRNA). The labeled cRNAs were hybridized onto Arraystar Human circRNA Arrays V2 (8x15 K; Arraystar, Inc.) and incubated for 17 h at 65˚C in an Agilent hybridization oven (Agilent Technologies, Inc.). After washing, the slides were scanned with the Agilent Scanner G2505C (Agilent Technologies, Inc.). Agilent Feature Extraction software (Version 11.0.1.1) was used to extract the data (Agilent Technologies, Inc.). Subsequently, the R software package 'limma' (16) was used to perform a series of data processing steps. After the original data was normalized, high-quality probes were screened. The probes were marked as present (P), marginal (M) or absent (A). In total, ≥ three of the six samples of circRNAs were flagged in 'P' or 'M' under 'All Targets Value', and these circRNAs were retained for improved differential analysis. A statistically significant difference (fold change >1.5) in expression of circRNAs was identified between two groups by multiple change cut-off or volcano plot filtration. The Arraystar proprietary miRNA target prediction software and TargetScan Human 7.2 (http://www.targetscan.org/vert_72/) were used to identify the potential interactions between circRNAs and their target microRNAs. TargetScan v7.2 and miRDB v5 were used to predict the target genes of these microRNAs. Using the overlapping data, three circRNAs were selected that were associated with COL1A1 and ELN for further qPCR verification. Gene Ontology (GO) annotation and KEGG pathway analysis were performed to provide evidence for the further functional prediction of the differentially expressed circRNAs. These circRNAs were input into the Database for Annotation, Visualization and Integrated Discovery (http://david.abcc.ncifcrf.gov/) and the KEGG database (http://www.genome.jp/kegg/). The P-values denote the significance of the GO term enrichment and the correlation of KEGG pathway (P<0.05 was considered to indicate a statistically significant result). The circRNA expression chip and bioinformatics data analyses were completed by Shanghai Kangcheng Biotechnology Co., Ltd.

RT-qPCR. Total RNA was isolated from the samples using the TRIzol® Plus RNA Purification kit (Thermo Fisher Scientific, Inc.), and its concentration and purity were determined using a NanoDrop 2000 spectrophotometer (Thermo Fisher Scientific, Inc.). Complementary (c)DNA was synthesized by reverse-transcribing 2 μg total RNA using the PrimeScript™ RT Reagent kit (Takara Bio, Inc.). cDNA was amplified according to the instructions of the TB Green Fast qPCR Mix (Takara Bio Inc.). The volume of the PCR amplification mixture was 20 μl, including 10 μl 2X qPCR SYBR®-Green Master Mix, 0.5 μl forward primer (10 μM), 0.5 μl reverse primer (10 μM), 1 μl cDNA and 8 μl RNase-free H_2O. The amplification conditions were as follows: Pre-denaturation at 95˚C for 5 min, followed by 40 cycles of denaturation at 95˚C for 10 sec and annealing at 60˚C for 34 sec. The relative expression was quantified using the $2^{-\Delta\Delta Cq}$ method (17), and GAPDH was used as an internal reference gene. Sequences of the primer pairs were listed in Table I.

Statistical analysis. The results are representative of three independent experiments and are presented as the mean ± standard error of the mean. Statistical analysis was performed using SPSS 20.0 statistical software (IBM Corp.). The F-test was used to test the homogeneity of variance. The independent samples Student's t-test was used to compare the means between the chronic UVA irradiation group and the unexposed control group. P<0.05 was considered to indicate a statistically significant difference.

Results

Verification of the skin fibroblast model of photoaging. A number of changes including increased SA-β-Gal activity and cell cycle-associated protein expression have been reported to be induced by UVA irradiation (18,19). Compared with that in the normal control group, the senescence staining was increased in the UVA-treated group (Fig. 1A). Western blot

Table I. Primer sequences of circular RNAs.

circBase ID	Sequence (5'-3')	Size, bp
hsa_circ_0006766-F	TGTTGCCATTACAGGGGTAAGT	146
hsa_circ_0006766-R	CGGGAAGGAAAGTGATATTTGG	
hsa_circ_0011129-F	CTTCCGGGCCCAGGTCCTTC	149
hsa_circ_0011129-R	AGTGCAGGCGCCAGAAGCTGG	
hsa_circ_0017502-F	CCAGATCATGCCAGGTGACAT	135
hsa_circ_0017502-R	TACGGAACTGCACGCTGAAC	
GAPDH-F	GACACCATGGGGAAGGTGAA	79
GAPDH-R	AGTTAAAAGCAGCCCTGGTG	

Circ, circular RNA; F, forward; R, reverse.

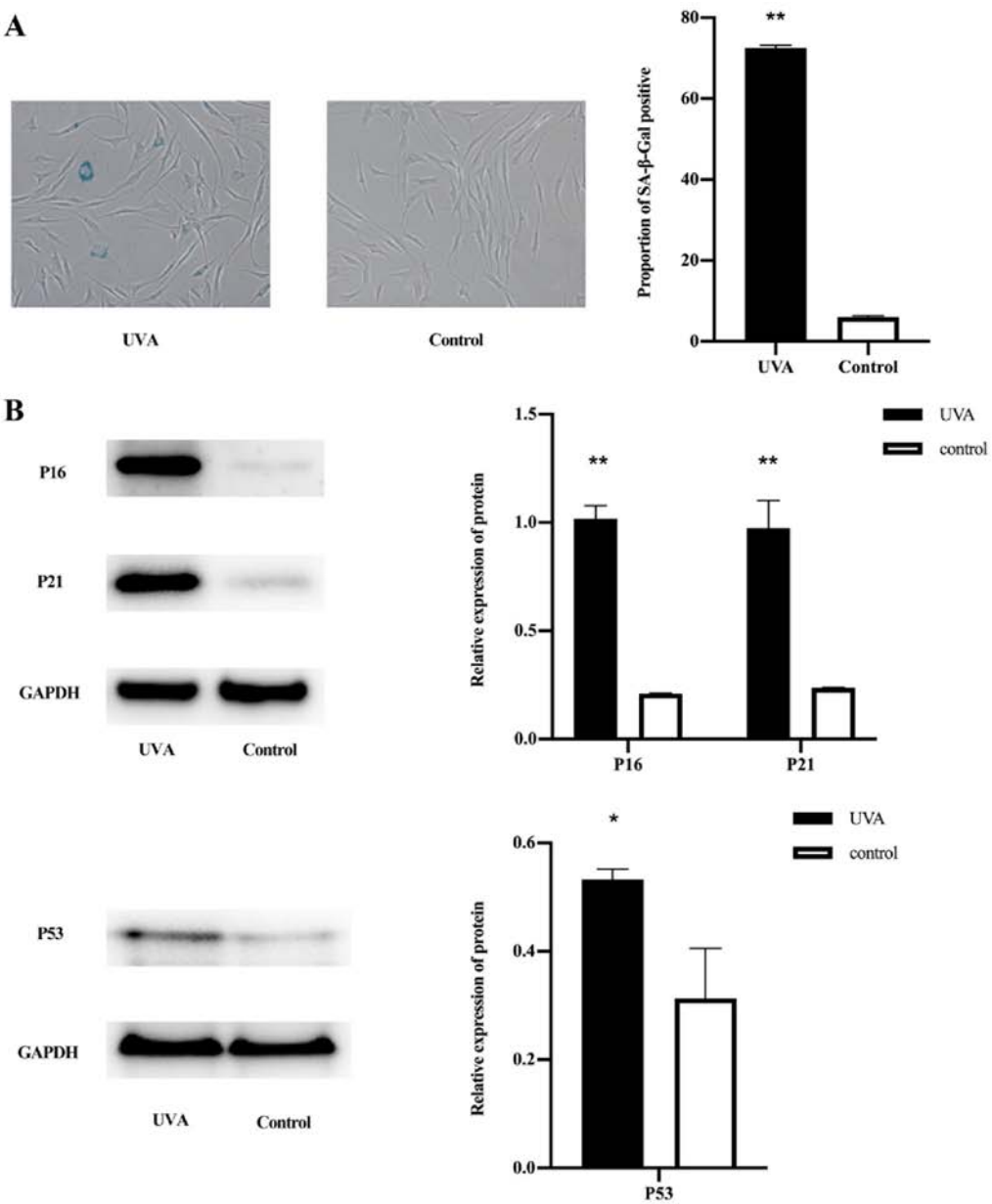

Figure 1. Verification of the UVA-induced fibroblast model of senescence. (A) The cells with blue stained cytoplasm were considered aged cells (magnification, x100). Cells were counted in six randomly chosen microscopic fields, and the percentage of cells positive for SA-β-Gal activity was calculated. (B) P16, P21 and P53 were used to detect the differences in the expression of senescence-associated proteins between the UVA-treated and control groups. GAPDH was used as an internal reference. Values were expressed as the mean ± standard error of the mean (n=3), and all experiments were performed in triplicate. *P<0.05, **P<0.01 vs. control. UVA, ultraviolet A; SA-β-Gal, senescence-associated β-galactosidase.

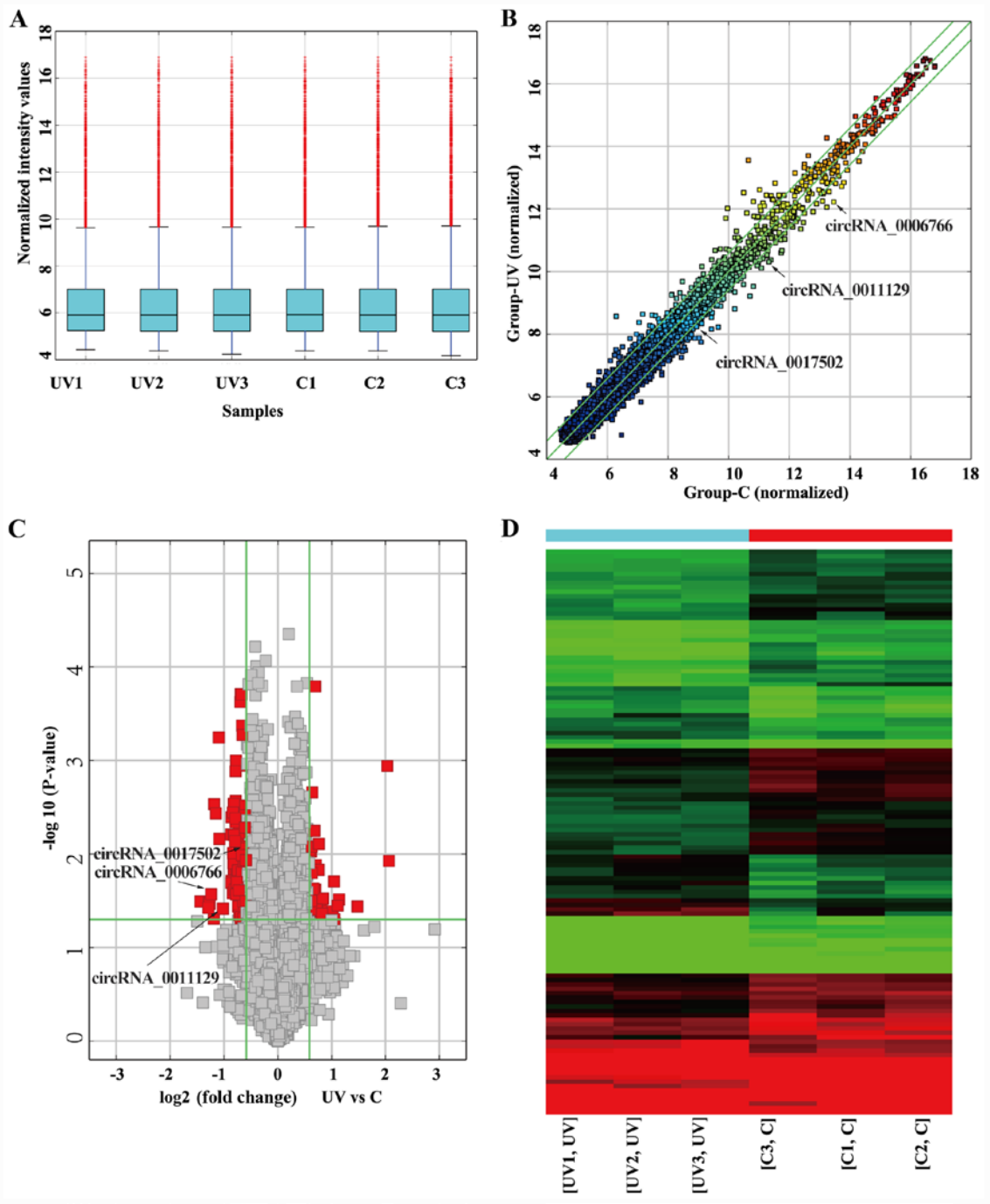

Figure 2. circRNA expression profile of fibroblasts after UVA irradiation. (A) The distribution of total circRNA expression between the UVA-treated and control groups was similar. (B) The scatter plot demonstrated the differences in circRNA expression between the UVA-treated and control groups. The green line is an FC line, and the difference in circRNA expression between the top green line and the bottom green line is >1.5-fold. (C) Volcano plot displaying circRNAs differentially expressed with statistical significance (FC>1.5; P<0.05). (D) Hierarchical clustering analysis of differentially expressed circRNAs between the UVA irradiation group and the control group. UVA, ultraviolet A; circRNA, circular RNA; FC, fold change; UV, UVA-treated group; C, control group.

analysis revealed that the expression of p16, p21 and p53 in the UVA-treated group was higher compared with that in the control group (Fig. 1B).

circRNA expression profiles in UVA-irradiated human dermal fibroblasts. A circRNA microarray was used to obtain the expression profiles of circRNAs in UVA-irradiated human dermal fibroblasts. The distribution of circRNA expression profiles exhibited no differences between the UVA-treated group and the non-irradiated control group (Fig. 2A). Differentially expressed circRNAs between two compared groups were identified through Fold Change filtering (Fig. 2B) or Volcano Plot filtering (Fig. 2C). In Fig. 2D, hierarchical clustering was utilized to show circRNA expression profiling among the all samples. The data showed that there was a distinctly distinguishable circRNAs expression profile between the UVA-treated group and non-irradiated group. Compared with the non-irradiated control group, 128 circRNAs were determined to be differentially expressed after UVA exposure based on the

Table II. circRNAs differentially expressed following ultraviolet A treatment.

A, Upregulated circRNAs

circRNA	FC (abs)	Gene symbol	P-value
hsa_circRNA_103065	4.1715	MYBL2	0.0118
hsa_circRNA_100445	4.0847	TATDN3	0.0011
hsa_circRNA_103361	2.7804	SMARCC1	0.0362
hsa_circRNA_000401	2.1920	BRD9	0.0305
hsa_circRNA_048148	2.1574	CNN2	0.0356
hsa_circRNA_104484	2.0623	ZC3HC1	0.0494
hsa_circRNA_404870	2.0559	METTL15	0.0197
hsa_circRNA_005411	2.0248	EXTL3	0.0407
hsa_circRNA_101093	1.7798	NUP107	0.0299
hsa_circRNA_092418	1.7606	B2M	0.0434

B, Downregulated circRNAs

circRNA	FC (abs)	Gene symbol	P-value
hsa_circRNA_101621	2.7131449	CEMIP	0.032211923
hsa_circRNA_007624	2.4404224	BCAR3	0.037482416
hsa_circRNA_004585	2.4282438	CEMIP	0.032890625
hsa_circRNA_000675	2.4117771	NDUFA10	0.034232964
hsa_circRNA_006766	2.3634626	CCL24	0.026828638
hsa_circRNA_100191	2.2776152	PTPRF	0.048836243
hsa_circRNA_004594	2.2729704	MLLT1	0.002923375
hsa_circRNA_102817	2.219963	SAP130	0.003660652
hsa_circRNA_062539	2.1416076	BCR	0.00056699
hsa_circRNA_104647	2.1249749	ZFHX4	0.006894599

circRNA, circular RNA; FC (abs), absolute fold-change.

criteria FC>1.5 and P<0.05, including 39 upregulated and 89 downregulated circRNAs. The top 20 aberrant circRNAs are listed in Table II.

GO and KEGG pathway analyses. To determine the roles of circRNAs in the physiology and pathology of fibroblasts after UVA irradiation, GO and KEGG pathway analyses of mRNAs transcribed from parental genes of the differentially expressed circRNAs were performed. The results demonstrated that the most significantly enriched relevant GO terms in the biological process category were 'collagen catabolic process' and 'collagen metabolic process', as well as 'extracellular matrix' (ECM; Fig. 3A). In the cellular component category, the parental genes of the differentially expressed circRNA were identified to be accumulated in the 'complex of collagen trimers' (Fig. 3B). In the molecular function category, the most significantly enriched terms were 'extracellular matrix structural construction', 'metalloendopeptidase' and 'protein binding' (Fig. 3C). KEGG pathway analysis revealed the top 10 pathways that may be involved in skin photoaging (Fig. 3D). Among these, the 'Age-RAGE signaling pathway in diabetic complications' had been reported to be involved in skin photoaging (20,21).

Verification of differentially expressed circRNAs by RT-qPCR. The main pathological changes of photoaging are the accumulation of abnormal elastin and a severe loss of collagen fibers in dermis (1,2). To verify the data of the circRNA microarray, three circRNAs that were predicted to be associated with collagen type I (COL1A1) and elastin (ELN) were selected to be confirmed by RT-qPCR analysis. There were no significant differences in the expression levels of circ-0017502, but there were significant downregulations in the expression levels of circ-0006766 and circ-0011129 in the UVA-irradiated group compared with those in the control group (Fig. 4). The expression pattern was similar to that obtained from the circRNA microarray.

Discussion

Accumulating evidence indicates UVA to be a major contributing factor in photoaging, but its mechanisms remain to be fully elucidated (1). Furthermore, UVA is associated with a variety of light-associated diseases, including skin cancer (4). Therefore, developing new markers for early diagnosis and the design of preventive strategies would be of benefit. Non-coding RNAs have been widely assessed in studies on gene function

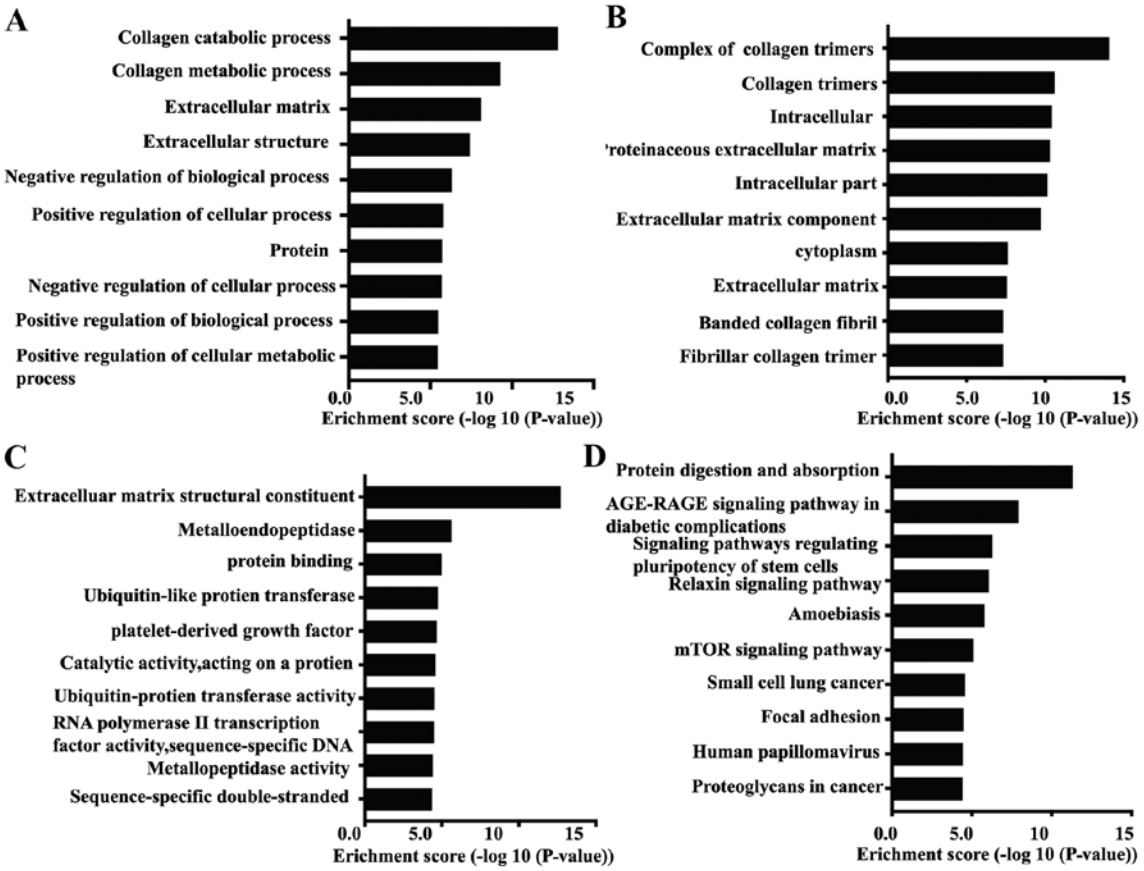

Figure 3. GO enrichment and pathway analysis derived of the host genes of the differentially expressed circRNAs. (A-C) GO terms in the categories (A) biological process, (B) cellular component and (C) molecular function. (D) Bar chart displaying the top 10 enriched pathways. GO, gene ontology.

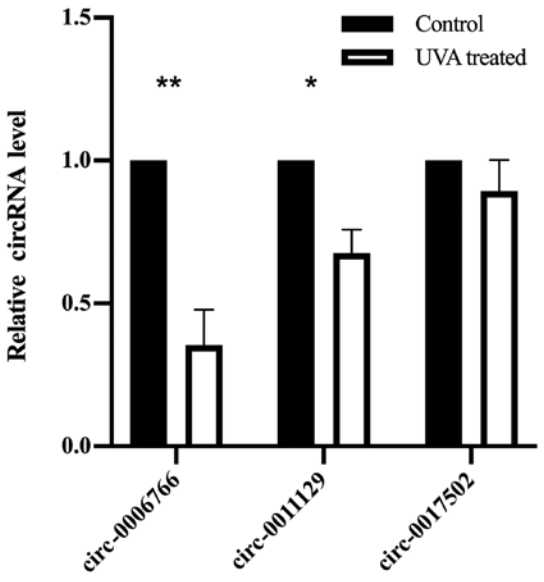

Figure 4. Reverse transcription-quantitative PCR verification results of three circRNAs. Quantitative PCR validation was performed on six samples for Circ-0006766, Circ-0011129 and Circ-0017502. Values are expressed as the mean ± standard error of the mean (n=3 per group). *P<0.05, **P<0.01 vs. control. Circ/circRNA, circular RNA.

and disease treatment. For example, MRX34, a microRNA (miRNA) mimic, has reached phase 1 studies in patients with advanced solid tumors, including hepatocellular carcinoma, pancreatic cancer and cholangiocarcinoma (22). miR-146a may serve as a promising therapeutic target for dengue (23). Wheatley *et al* (24) previously developed a DNA vaccine vector co-expressing an miRNA designed *in silico* miRNA to inhibit PERK with a HIV-1 envelope. In the field of skin photoaging, non-coding RNA has also received increasing attention. For instance, downregulation of miR-34c-5p may inhibit the p53 pathway by increasing the level of the downstream target E2F transcription factor 3 and ultimately impair cell senescence (25). However, miRNAs and lncRNAs have a linear structure, due to which their stability is insufficient to withstand treatment with RNase (the 3' exonuclease of hydrolyzable linear RNAs) (26), limiting their clinical application. Compared with linear non-coding RNAs such as miRNAs and lncRNAs, circRNAs have the advantage of being more stable (9,27).

The role of circRNAs in photoaging remains to be fully elucidated. Previous studies by our group have indicated that circCOL3A1-859267, which targets miR-29c, is able to regulate the expression of type I collagen in fibroblasts (19,28). In the present study, the expression profile of circRNAs in UVA-irradiated fibroblasts was determined, and 128 differentially expressed circRNAs (FC>1.5 and P<0.05) were identified, including 39 upregulated and 89 downregulated circRNAs. GO and KEGG analyses indicated that the aberrant circRNAs were implicated in ECM organization and metabolism. Subsequently, RT-qPCR was used to verify three differentially expressed circRNAs and the results were similar to those of the circRNA microarray. Of note, the differentially

expressed circRNAs identified in the present study require further assessment by bioinformatics analyses and *in vivo* and *in vitro* experiments. For instance, the aberrant accumulation of ELN and the extensive loss of collagen fibers in dermis are the fundamental pathological changes of skin photoaging (29). Through the Arraystar proprietary miRNA target prediction software and TargetScan, the present study identified that the miRNAs that circ-0011129 may sponge, including hsa-miR-484, hsa-miR-3619-5p and hsa-miR-6732-5p, share binding sites with photoaging-related proteins, such as collagen type I α1 (COL1A1), COL3A1 or elastin.

Zhang *et al* (30) previously revealed that miR-6732-5p was one of seven significantly upregulated miRNAs in atypical meningioma patients that are resistant to radiotherapy, where the differentially expressed miRNAs were enriched mostly in the transforming growth factor-β (TGF-β) signaling pathway. In addition, Quan *et al* (31) revealed that UV irradiation impaired the TGF-β/Smad pathway in human dermal fibroblasts, thereby downregulating the expression of TGF-β target genes such as type I procollagen. Type I collagen is one of the main components of the dermal extracellular matrix. Extensive degradation of type I collagen is a fundamental pathological change of skin photoaging (1). Therefore, circ-0011129 is hypothesized to regulate the expression of type I collagen by targeting the miR-6732-5p and TGF-β/Smad pathway.

Several limitations of the present study should be acknowledged. The effect of ultraviolet A (UVA) on fibroblasts was explored but not ultraviolet B (UVB). Although both UVA and UVB are involved in skin photoaging, UVA penetrates deeper than UVB and induces more profound alterations in the dermal connective tissue (31,32). Therefore, for fibroblasts in the dermis, UVA has a greater impact. In addition, regulatory mechanisms of the differentially expressed circRNAs on photoaging remain to be fully elucidated, which serve to be the next step in this research.

In conclusion, the present study provided a unique circRNA profile in UVA-irradiated fibroblasts. These altered circRNAs may provide an avenue to elucidate the mechanisms of skin photoaging, as well as facilitate the development of small molecules to prevent and treat photoaging and associated skin diseases.

Acknowledgements

Not applicable.

Funding

The present study was supported by a grant from the National Natural Science Foundation of China (grant no. 81673047).

Availability of data and materials

The datasets used and/or analyzed during the present study are available from the corresponding author on reasonable request.

Authors' contributions

WL proposed the experimental concept and designed the study. ML and YZ established the UVA irradiation model and were major contributors in writing the manuscript. ML, QL, YL, QX and YL performed the microarray data analysis and performed critical data analyses. All authors read and approved the final manuscript.

Ethics approval and consent to participate

Informed written consent of patients' parents was obtained prior to tissue resection. The present study and all procedures were approved by the Medical Ethics Committee of the Third Affiliated Hospital of Sun Yat-sen University [no. (2016)2-63].

Patient consent for publication

Not applicable.

Competing interests

The authors declare that they have no competing interests.

References

1. Gilchrest BA: Photoaging. J Invest Dermatol 133: E2-E6, 2013.
2. Weihermann AC, Lorencini M, Brohem CA and de Carvalho CM: Elastin structure and its involvement in skin photoaging. Int J Cosmet Sci 39: 241-247, 2017.
3. Schneider SL and Lim HW: Review of environmental effects of oxybenzone and other sunscreen active ingredients. J Am Acad Dermatol 80: 266-271, 2018.
4. Burke KE: Mechanisms of aging and development-a new understanding of environmental damage to the skin and prevention with topical antioxidants. Mech Ageing Dev 172: 123-130, 2017.
5. Ma DL and Vano-Galvan S: Actinic Granuloma. N Engl J Med 376: 475, 2017.
6. Xie HF, Liu YZ, Du R, Wang B, Chen MT, Zhang YY, Deng ZL and Li J: MiR-377 induces senescence in human skin fibroblasts by targeting DNA methyltransferase 1. Cell Death Dis 8: e2663, 2017.
7. Li M, Li L, Zhang X, Zhao H, Wei M, Zhai W, Wang B and Yan Y: LncRNA RP11-670E13.6, interacted with hnRNPH, delays cellular senescence by sponging microRNA-663a in UVB damaged dermal fibroblasts. Aging (Albany NY) 11: 5992-6013, 2019.
8. Kristensen LS, Andersen MS, Stagsted LVW, Ebbesen KK, Hansen TB and Kjems J: The biogenesis, biology and characterization of circular RNAs. Nat Rev Genet 20: 675-691, 2019.
9. Guo JU, Agarwal V, Guo H and Bartel DP: Expanded identification and characterization of mammalian circular RNAs. Genome Biol 15: 409, 2014.
10. Memczak S, Jens M, Elefsinioti A, Torti F, Krueger J, Rybak A, Maier L, Mackowiak SD, Gregersen LH, Munschauer M, *et al*: Circular RNAs are a large class of animal RNAs with regulatory potency. Nature 495: 333-338, 2013.
11. Wang K, Long B, Liu F, Wang JX, Liu CY, Zhao B, Zhou LY, Sun T, Wang M, Yu T, *et al*: A circular RNA protects the heart from pathological hypertrophy and heart failure by targeting miR-223. Eur Heart J 7: 2602-2611, 2016.
12. Chen J, Li Y, Zheng Q, Bao C, He J, Chen B, Lyu D, Zheng B, Xu Y, Long Z, *et al*: Circular RNA profile identifies circPVT1 as a proliferative factor and prognostic marker in gastric cancer. Cancer Lett 388: 208-219, 2017.
13. Dube U, Del-Aguila JL, Li Z, Budde JP, Jiang S, Hsu S, Ibanez L, Fernandez MV, Farias F, Norton J, *et al*: An atlas of cortical circular RNA expression in Alzheimer disease brains demonstrates clinical and pathological associations. Nat Neurosci 22: 1903-1912, 2019.
14. Chen FG, Zhang WJ, Bi D, Liu W, Wei X, Chen FF, Zhu L, Cui L and Cao Y: Clonal analysis of nestin(-) vimentin(+) multipotent fibroblasts isolated from human dermis. J Cell Sci 120: 2875-2883, 2007.
15. Lamore SD and Wondrak GT: UVA causes dual inactivation of cathepsin B and L underlying lysosomal dysfunction in human dermal fibroblasts. J Photchem Photobiol B 123: 1-12, 2013.

16. Ritchie ME, Phipson B, Wu D, Hu Y, Law CW, Shi W and Smyth GK: limma powers differential expression analyses for RNA-sequencing and microarray studies. Nucleic Acids Res 43: e47, 2015.
17. Livak K and Schmittgen T: Analysis of relative gene expression data using real-time quantitative PCR and the 2(-Delta Delta C(T)) method. Methods 25: 402-408, 2000.
18. Park YM and Park SN: Inhibitory effect of lupeol on MMPs expression using aged fibroblast through repeated UVA Irradiation. Photochem Photobiol 95: 587-594, 2019.
19. Peng Y, Song X, Zheng Y, Cheng H and Lai W: circCOL3A1-859267 regulates type I collagen expression by sponging miR-29c in human dermal fibroblasts. Eur J Dermatol 28: 613-620, 2018.
20. Bouchie A: First microRNA mimic enters clinic. Nat Biotechnol 31: 577, 2013.
21. Farrar MD: Advanced glycation end products in skin ageing and photoageing: What are the implications for epidermal function? Exp Dermatol 25: 947-948, 2016.
22. Beg MS, Brenner AJ, Sachdev J, Borad M, Kang YK, Stoudemire J, Smith S, Bader AG, Kim S and Hong DS: Phase I study of MRX34, a liposomal miR-34a mimic, administered twice weekly in patients with advanced solid tumors. Invest New Drugs 35: 180-188, 2017.
23. Wong RR, Abd-Aziz N, Affendi S and Poh CL: Role of microRNAs in antiviral responses to dengue infection. J Biomed Sci 27: 4, 2020.
24. Wheatley AK, Kramski M, Alexander MR, Toe JG, Center RJ and Purcell DF: Co-expression of miRNA targeting the expression of PERK, but not PKR, enhances cellular immunity from an HIV-1 Env DNA vaccine. PLoS One 6: e18225, 2011.
25. Zhou BR, Guo XF, Zhang JA, Xu Y, Li W, Wu D, Yin ZQ, Permatasari F and Luo D: Elevated miR-34c-5p mediates dermal fibroblast senescence by ultraviolet irradiation. Int J Biol Sci 9: 743-752, 2013.
26. Ivanov A, Memczak S, Wyler E, Torti F, Porath HT, Orejuela MR, Piechotta M, Levanon EY, Landthaler M, Dieterich C, *et al*: Analysis of intron sequences reveals hallmarks of circular RNA biogenesis in animals. Cell Rep 10: 170-177, 2015.
27. You X, Vlatkovic, Babic A, Will T, Epstein, Tushev G, Akbalik G, Wang M, Glock C, Quedenau C, *et al*: Neural circular RNAs are derived from synaptic genes and regulated by development and plasticity. Nat Neurosci 18: 603-910, 2015.
28. Peng Y, Song X, Zheng Y, Wang X and Lai W: Circular RNA profiling reveals that circCOL3A1-859267 regulate type I collagen expression in photoaged human dermal fibroblasts. Biochem Biophys Res Commun 486: 277-284, 2017.
29. Xu D, Li D, Zhao Z, Wu J and Zhao M: Regulation by walnut protein hydrolysate on the components and structural degradation of photoaged skin in SD rats. Food Funct 10: 6792-6802, 2019.
30. Zhang X, Zhang G, Huang H, Li H, Lin S and Wang Y: Differentially expressed MicroRNAs in radioresistant and radiosensitive atypical meningioma: A clinical study in chinese patients. Front Oncol 10: 501, 2020.
31. Quan T, He T, Kang S, Voorhees JJ and Fisher GJ: Solar ultraviolet irradiation reduces collagen in photoaged human skin by blocking transforming growth factor-beta type II receptor/Smad signaling. Am J Pathol 165: 741-751, 2004.
32. Battie C, Jitsukawa S, Bernerd F, Del Bino S, Marionnet C and Verschoore M: New insights in photoaging, UVA induced damage and skin types. Exp Dermatol 23 (Suppl 1): 7-12, 2014.